

## Seismic response of geosynthetic reinforced retaining walls

Mehrab Jesmani<sup>1a</sup>, Mehrad Kamalzare<sup>\*2</sup> and Babak Bahrami Sarbandi<sup>3b</sup>

<sup>1</sup> Department of Civil Engineering, Imam Khomeini International University, Ghazvin, Iran

<sup>2</sup> Department of Civil and Environmental Engineering, Rutgers University, Piscataway, NJ, USA

<sup>3</sup> Department of Civil Engineering, Islamic Azad University, Arak, Iran

(Received July 06, 2015, Revised January 22, 2016, Accepted February 11, 2016)

**Abstract.** The effects of reinforcement on the horizontal and vertical deformations of geosynthetic reinforced retaining walls are investigated under a well-known seismic load (San Jose earthquake, 1955). Retaining walls are designed with internal and external stability (with appropriate factor of safety) and deformation is chosen as the main parameter for describing the wall behavior under seismic load. Retaining walls with various heights (6, 8, 10, 12 and 14 meter) are optimized for geosynthetics arrangement, and modeled with a finite element method. The stress-strain behavior of the walls under a well-known loading type, which has been used by many previous researchers, is investigated. A comparison is made between the reinforced and non-reinforced systems to evaluate the effect of reinforcement on decreasing the deformation of the retaining walls. The results show that the reinforcement system significantly controls the deformation of the top and middle of the retaining walls, which are the critical points under dynamic loading. It is shown that the optimized reinforcement system in retaining walls under the studied seismic loading could decrease horizontal and vertical deformation up to 90% and 40% respectively.

**Keywords:** reinforced soils; retaining walls; geosynthetic; seismic load; numerical method

---

### 1. Introduction

Steel belt reinforced soil was introduced by a French engineer, Vidal (1966) to the geotechnical engineering society as the first reinforced earth system. This became the basis for initial research in this field. During 1970s, many tests performed on different materials, which drew the researchers' attention to the use of geotextiles. Finally, a method of soil reinforcement by using geotextiles was introduced by a Swedish geotechnical group. The design methods innovated at that time for reinforcement systems by Lee *et al.* (1973) for steel reinforcement and by Bell *et al.* (1975) for textile reinforcements, became the base for designing methods. These design methods, which were according to Rankine's theory, were developed by Koerner (1986). In his developed method, a part of the active weight of the soil in the back of retaining structure was being used against lateral pressure of soil as the resistance factor. It led to saving in materials consumption and making the system more economical, particularly in the protection of high trenches in

---

\*Corresponding author, Adjunct Professor, Registered Professional Engineer in the State of Connecticut, USA, E-mail: [mehrad\\_k@yahoo.com](mailto:mehrad_k@yahoo.com); [m.kamalzare@rutgers.edu](mailto:m.kamalzare@rutgers.edu)

<sup>a</sup> Associate Professor, Registered Professional Engineer in the State of California, USA

<sup>b</sup> M.Sc., E-mail: email address

transportation and road structure projects. In the meantime, failure happened slowly, which was another advantage of this reinforcement system, in contrast to the sudden destructions of other methods. The structural and economical superiority of this system was significantly considerable compared to unreinforced retaining walls. It should be noted that the reinforced steep slopes (RSS), which make an angle of 70 to 90 degrees with horizontal line, are common slopes in road and railroad projects and are classified in the reinforced retaining walls (or generally Mechanically Stabilized Earth Walls, MSEW). For their external face, a thin coating could be used to protect the geotextile against atmospheric and environmental destruction such as disintegration against ultraviolet lights.

The reinforced retaining walls have been an interesting topic for researchers, and significant investigations have been done on this topic. To compensate for low number of behavioral observations in slope and reinforced walls under seismic load, a number of experimental tests were performed in the last few years on a small scale by using a vibrating table and centrifuge. At the same time, observing and studying the behavior of the tested reinforced walls in the seismic places generally provides the initial data for modeling reinforcement systems. New generations of these tests and studies are introduced in papers published in recent years. Ismeik and Shaqour (2015) presented a theoretical derivation of a new analytical formulation for estimating magnitude and lateral earth pressure distribution on a retaining wall subjected to seismic loads. Their proposed solution accounted for failure wedge inclination, unit weight and friction angle of backfill soil, wall roughness, and horizontal and vertical seismic ground accelerations. A parametric study was also conducted to examine the influence of various parameters on lateral earth pressure distribution. Findings revealed that lateral earth pressure increases with the increase of horizontal ground acceleration while it decreases with the increase of vertical ground acceleration. Zheng *et al.* (2015) presented an analytical solution for active earth pressures on retaining structures of cohesive backfill with an inclined surface subjected to surcharge, pore water pressure and seismic loadings. The investigation was on the basis of the lower-bound theorem of limit analysis combined with Rankine's earth pressure theory and the Mohr-Coulomb yield criterion. The generalized active earth pressure coefficients (dimensionless total active thrusts) were presented for use in comprehensive design charts.

The existing design standards such as National Concrete Masonry Association (NCMA), AASHTO and Federal Highway Administration (FHWA), use the pseudo-static analysis to design the structures against seismic load. This method works by merely multiplying some coefficients to the dead weights, and modeling and analyzing the earthquake statically. Peak Ground Acceleration (PGA), which is used in this method is not a detailed and fully proper parameter for simulating the effects of dynamic movement of ground in the earthquake and the applying loads to the structure. There are some other methods like European design method, which have different details. However, in the present research, FHWA method is used for initial design of geotextiles as it is more common in engineering practice. Also, in the conventional design of retaining structures in a seismic zone, seismic inertia forces are commonly assumed to act upwards and towards the wall facing to cause a maximum active thrust or act upwards and towards the backfill to cause a minimum passive resistance. However, under certain circumstances this design approach might underestimate the dynamic active thrust or overestimate the dynamic passive resistance acting on a rigid retaining structure. Nian *et al.* (2014) developed a new analytical method for dynamic active and passive forces in  $c-\phi$  soils with an infinite slope was proposed based on the Rankine earth pressure theory and the Mohr-Coulomb yield criterion, to investigate the influence of seismic inertia force directions on the total active and passive forces. The results of the study showed that a

combination of downward and towards-the-wall seismic inertia forces causes a maximum active thrust while a combination of upward and towards-the-wall seismic inertia forces causes a minimum passive resistance. Gazetas *et al.* (2004) and Jesmani *et al.* (2011), used finite element modeling to explore the magnitude and distribution of dynamic earth pressures on several types of flexible retaining systems. The utilized base excitation was typical of earthquake motions of either high or moderately low dominant frequencies having peak ground acceleration (PGA) of 0.40 g and relatively short duration. The results showed that as the degree of realism in the analysis increases, the frequently observed satisfactory performance of such retaining systems during strong seismic shaking could be explained.

Bathurst *et al.* (2005) developed a new working stress method for the calculation of reinforcement loads in geosynthetic reinforced soil walls. Careful back-analyses of a database of instrumented and monitored full-scale field and laboratory walls were used to demonstrate that the current American Association of State Highway and Transportation Officials (AASHTO) Simplified Method used in North America results in excessively conservative estimates of the volume of reinforcement required generating satisfactory long-term wall performance. The new design method captured the essential contributions of the different wall components and properties to reinforcement loads. Jesmani *et al.* (2010) studied the effects of plasticity and normal stress on undrained shear modulus of clayey soils. GuhaRay and Baidya (2014) presented a possible framework for obtaining the partial safety factors based on reliability approach for different random variables affecting the stability of a reinforced concrete cantilever retaining wall and a slope under static loading conditions. Reliability analysis was carried out by Mean First Order Second Moment Method, Point Estimate Method, Monte Carlo Simulation and Response Surface Methodology. The importance of partial safety factors was shown by analyzing two simple geotechnical structures. Ji and Liao (2014) studied a sensitivity-based reliability analysis of earth slopes using finite element method, and proposed a new procedure. El-Emam and Bathurst (2007) studied the influence of reinforcement design parameters (i.e., stiffness, length and vertical spacing) on the simulated earthquake response of reinforced soil retaining walls using reduced-scale model shaking table tests. The reinforcement design parameters investigated were found to have a significant effect on model response. Experimental results showed that the magnitude of accumulated facing lateral displacement under base excitation decreased with increasing reinforcement length, greater number of reinforcement layers and larger reinforcement stiffness. However, the measured vertical load at the footing was not significantly influenced by changes in reinforcement parameters. Yoo and Kim (2008) presented the results of a full-scale load test and a 3D finite element analysis on a two-tier, 5 m high, geosynthetic reinforced segmental retaining wall (GR-SRW) subjected to a surcharge load aiming at investigating the response of the GR-SRW to various levels of surcharge load. The results of the load test at working stress condition revealed that the GR-SRW's response to the test load was well within the serviceability limits, and that the currently available design guideline tends to over-estimate the surcharge load-induced reinforcement forces. The predicted results for the surcharge load well in excess of the test load indicated that the surcharge load-induced reinforcement strains exponentially decrease with depth, showing a good agreement in qualitative terms with that assumed in the FHWA design guideline. Sabermahani *et al.* (2009) conducted a series of 1-g shaking table tests. The effects of parameters such as soil density, reinforcement length, spacing and stiffness on the seismic response of the model walls were studied. Different deformation modes (overturning and bulging) of the facing as well as base sliding were observed. Based on the results of physical model testing, it was concluded that reinforcement stiffness is a key parameter dominating the seismic response and

deformation mode of a wall and not reinforcement ultimate tensile strength, which is currently used as the main parameter for wall design in existing codes.

One of the main purpose of this research was to evaluate the seismic response of the geosynthetic reinforced retaining walls in comparison to non-reinforced ones, and to investigate and demonstrate the role of the reinforcements in controlling the deformations and limiting the displacements of retaining walls to the acceptable ranges. For this purpose, a well-known and well-studied earthquake load (San Jose earthquake) was used and a finite element method was developed to investigate this matter. Five clayey retaining walls with conventional heights in civil engineering and road projects were considered in the course of this research to provide more realistic results. The walls were designed with internal and external stability under static load (with appropriate factor of safety) and a reinforcing system of geotextile was designed for each of them based on the Bell *et al.* (1975) method. Numerical models of these retaining walls were created and their stability under earthquake loading was investigated. However, all walls were not completely stable according to first reinforcement design. Therefore, in order to find the most suitable reinforcing system for each wall, the length of geotextiles increases for unstable walls, and new models were created analyzed. To avoid the unnecessary complication of the models and to shorten the analyses time, vertical space between geotextiles was assumed constant. New analyses with new length of geotextiles for each wall were performed until a factor of safety between 1 and 1.2 (suitable amount of factor of safety based on the pseudo-static analysis method) was obtained. At last, horizontal and vertical displacement of walls under the earthquake load were studied. Deformation was chosen as the main parameter for describing the wall behavior under seismic load. Finally, diagrams and tables are presented to evaluate and determine the amounts of horizontal and vertical displacements at different levels of the retaining wall in non-reinforced and reinforced conditions, and the relevant mathematical formulas are introduced.

## 2. Design of reinforced retaining walls

Increasing the usage of reinforced retaining walls has led to innovating and introducing different design methods. Studying and comparing these methods indicate that a suitable design method should consist following stages (Holtz and Lee 2002):

- Analysis of stress under service loads
- Analysis of limit equilibrium (internal and external stability)
- Evaluation of deformations.

Stress analysis leads to an alternative for reinforcement position in the reinforced mass, and at the same time, it demonstrates the local stability of the mass at different levels of reinforcement. The limit equilibrium analysis controls the total stability (both internal and external) of the reinforced mass. In controlling the external stability, the reinforced mass is considered monolith and different failure planes in various forms examine the general destruction of the reinforced mass. In analysis of internal stability, it is assumed that the failure planes occur inside the reinforced mass. It should be mentioned that in some cases, the critical plane of partial fracture occurs inside the reinforced body and in others it would take place outside of it (Elias *et al.* 2001).

In analyzing the reinforced retaining walls under dynamic loading (e.g., earthquake and explosion), application of pseudo-static method is conventional. The design methods are based on the maximum horizontal acceleration of the earthquake, which is related to the region and zone of

the study. In assessing external stability, an additional lateral force would be applied to the reinforced wall from the soil, and at the same time, the mass of the reinforced body is affected by the lateral inertia forces (Day 2002). In other words, in common design methods, pseudo-static analysis is used for such loadings, and by using the Mononobe-Okabe method, a factor related to the maximum lateral acceleration of the earthquake would be applied to the dynamic load and change it to the equivalent static load, which would accordingly be applied to the wall (Okabe 1924). In order to study the internal stability, numerical methods and pseudo-static analysis is used. The force being applied on each layer of reinforcement is estimated, and pulling out and rupturing is controlled (Fig. 1). According to this approach and by using Eq. (1), the maximum stable height of the vertical retaining walls in static status with suitable safety factor is obtained for five types of clay soils, their properties are shown in Table 1. In this table, E represents module of elasticity,  $\phi_u$  is undrained friction angle and  $c_u$  is undrained cohesion

$$H_{cr} = \frac{4c_u}{\gamma} \left[ \frac{\cos \phi_u}{1 - \sin \phi_u} \right] \tag{1}$$

where:

- $c_u$  : Cohesion of soil
- $\phi_u$  : Internal frictional angle
- $\gamma$  : Density of the soil
- $H_{cr}$  : Critical height of the wall
- $SF$  : Safety factor
- $H$  : Height of the wall according to appropriate safety factor

It is important to mention that these parameters were selected based on fully natural conditions of unsaturated clay, which contains an amount of granular particles. One of the most important steps in simulating a real problem by a numerical method is to simulate realistic soil parameters

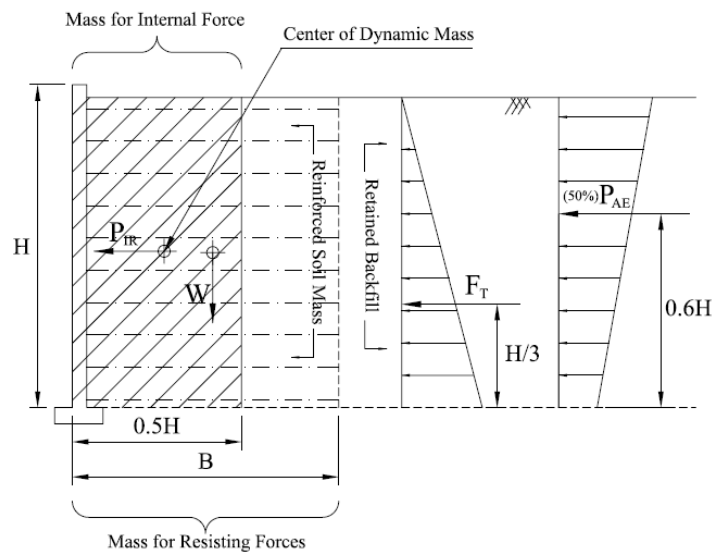


Fig. 1 Pseudo-static loading of reinforced retaining wall according to Mononobe-Okabe Method

that correspond to field conditions. The pertinent properties of clayey soils were selected based on the common values in practical projects and records related to some soil investigation. The soil parameters were chosen in range of the moderate and prevalent values of natural clay soils specification. The Liquid limit and Plastic Index of clay soils were between 30 and 55, and 18 and 35 respectively, and the soils contained about 15% of granular particles (sand) which according to Unified Soil Classification System (USCS) it was classified as CL or CH.

To reinforce retaining walls in relatively optimized conditions, various types of geotextiles with tensional resistances between 45 kN/m and 105 kN/m were used with respect to the height of the wall. The specifications of selected geotextiles for each retaining wall are listed in Table 2. However, the thickness of all geotextiles is considered 1cm, the maximum strain, 10%, mesh size, 0.07 mm, and the water permeability normal to the plane has been assumed 0.3 lit/m<sup>2</sup>s for each geotextile.

Trial-error method was used in order to design geotextiles and to reach the desire stability against the seismic load. First, by using the Bell *et al.* (1975) method, the plans of geotextiles along with the safety factor against rupture  $FS$  (B) as well as safety factor against pull out  $FS$  (P) were presented for stability of the retaining wall against dynamic loading of San Jose earthquake.

These plans were replicated by finite element modeling, and a dynamic load similar to San Jose earthquake was applied to them. Each time in the case of instability of the wall, another design of geotextiles was modeled by considering higher safety factor ( $FS$  (B) and  $FS$  (P)). This procedure was repeated until the model became stable and the desired safety factor ( $FS$  between 1 and 1.2, which is the suitable amount of factor of safety based on the pseudo-static analysis method) was obtained. It is worthwhile to mention that a seismograph apparatus and an accelerometer, which had recorded the San Jose earthquake, were placed in a very close distance to the earthquake center (approximately 12 km away), and the spectrum of the earthquake were recorded with high precision. Therefore, this earthquake load has been considered by many researchers, and has been the basis of several studies. It should be also noted that ANSYS is widely used software in

Table 1 Properties of the soil and retaining walls

$H$ (m)	S.F.	$H_{cr}$ (m)	$E$ (MN/m <sup>2</sup> )	$\gamma$ (kN/m <sup>3</sup> )	$\phi_u^\circ$	$c_u$ (kN/m <sup>2</sup> )
6	1.19	7.15	30	20	10	30
8	1.19	9.53	40	20	10	40
10	1.19	11.92	50	20	10	50
12	1.19	14.30	60	20	10	60
14	1.19	16.68	70	20	10	70

Table 2 Properties of geotextiles reinforcement

$H$ (m)	Mass per unit area (g/m <sup>2</sup> )	Tensile strength (kN/m)
6	170	45
8	250	60
10	300	70
12	500	125
14	400	105

defining several contact elements. It has good capabilities for modeling reinforced soil and determining the contact behavior between soils and reinforcing elements. In addition, since load-stretch curve is an important issue in geotextile reinforced walls, a certain definition of changes in tensional stress along with the variation of length was considered in the model.

The designed geotextiles for retaining walls with different heights (6, 8, 10, 12 and 14 meters), which are under dynamic load of San Jose earthquake are listed in Tables 3 to 7. Fig. 2 shows

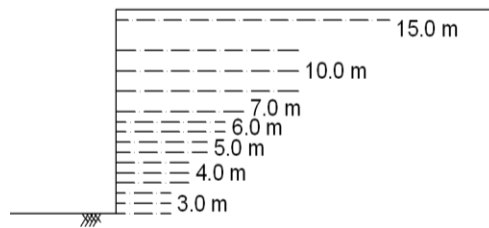


Fig. 2 Vertical cross section of 10-meter reinforced retaining wall

Table 3 The design of geotextile for 6-meter retaining wall under San Jose Earthquake loads

Z	$S_V$	L	FS (B)	FS (P)
1.50	1.50	12.00	3.55	4.50
2.50	1.00	7.00	3.19	3.37
3.40	0.90	6.00	2.61	3.521
4.10	0.70	5.00	2.78	4.04
4.70	0.60	4.00	2.83	4.02
5.30	0.60	3.00	2.23	3.33
5.65	0.35	2.00	4.03	4.04
6.00	0.30	1.00	3.80	3.55

Table 4 The design of geotextile for 8-meter retaining wall under San Jose Earthquake loads

Z	$S_V$	L	FS (B)	FS (P)
1.50	1.50	13.00	4.70	4.17
2.50	1.00	10.00	4.26	4.46
3.50	1.00	8.00	3.04	3.50
4.30	0.80	7.00	3.09	4.04
5.00	0.70	6.00	3.04	4.12
5.60	0.60	5.00	3.17	3.43
6.10	0.50	4.00	3.49	3.99
6.60	0.50	4.00	3.22	4.68
7.10	0.50	3.00	3.00	3.72
7.55	0.45	2.00	3.13	3.00
8.00	0.45	1.00	3.00	3.68

Table 5 The design of geotextile for 10-meter retaining wall under San Jose Earthquake loads

$Z$	$S_V$	$L$	$FS (B)$	$FS (P)$
1.50	1.50	15.00	5.12	4.35
2.50	1.00	10.11	4.61	3.07
3.50	1.00	10.00	3.30	3.77
4.50	1.00	10.00	3.00	4.46
5.00	0.50	7.00	4.61	4.67
5.50	0.50	6.00	4.20	3.00
6.00	0.50	6.00	3.85	4.38
6.60	0.50	5.00	3.55	3.42
7.00	0.50	5.00	3.30	4.12
7.50	0.50	4.00	3.10	3.15
8.00	0.50	4.00	3.00	3.85
8.50	0.50	4.00	2.70	4.55
9.00	0.50	3.00	2.65	3.58

Table 6 The design of geotextile for 12-meter retaining wall under San Jose Earthquake loads

$Z (m)$	$S_V (m)$	$L (m)$	$FS (B)$	$FS (P)$
2.00	2.00	20.00	5.55	4.82
3.50	2.00	15.00	4.23	4.34
4.50	1.00	12.00	4.93	4.73
5.50	1.00	12.00	4.03	5.43
6.50	1.00	12.00	3.41	6.13
7.30	0.80	10.00	3.80	6.24
8.00	0.70	8.00	3.96	5.51
8.50	0.50	6.00	5.22	5.03
9.00	0.50	6.00	4.93	5.78
9.50	0.50	5.00	4.67	4.82
10.00	0.50	5.00	4.44	5.51
10.40	0.40	3.50	5.33	4.47
10.80	0.40	3.00	5.13	4.13
11.20	0.40	3.00	4.95	4.83
11.60	0.40	2.50	4.78	4.50
12.00	0.40	2.50	4.62	5.18

a scheme of the design for a 10-meter retaining wall as an example. Unlike conventional designing methods that use same lengths for reinforcement for simplification, the result of present design suggests a triangle system to satisfy both the analysis conditions and optimized design, and it is also adoptive to general approach of Rankine method ( $45 + \varphi/2$ ).

Table 7 The design of geotextile for 14-meter retaining wall under San Jose Earthquake loads

$Z$ (m)	$S_v$ (m)	$L$ (m)	$FS$ (B)	$FS$ (P)
1.80	1.80	25	5.75	6.81
3.00	1.20	18	5.18	6.50
4.00	1.00	15.5	4.66	5.89
5.00	1.00	14.50	3.73	5.77
5.80	0.80	12.00	4.01	5.31
6.60	0.80	12.00	3.53	6.00
7.30	0.70	10.00	3.65	5.18
8.00	0.70	10.00	3.32	5.88
8.50	0.50	8.00	4.38	5.61
9.00	0.50	8.00	4.14	6.31
9.50	0.50	8.00	3.92	7.00
10.00	0.50	7.00	3.73	6.05
10.40	0.40	6.00	4.48	6.14
10.80	0.40	5.00	4.31	5.00
11.20	0.40	5.00	4.16	5.50
11.60	0.40	5.00	4.00	6.18
12.00	0.40	5.00	3.88	6.88
12.40	0.40	4.00	3.75	5.51
12.80	0.40	4.00	3.64	6.21
13.10	0.30	3.00	4.74	6.20
13.40	0.30	3.00	4.63	6.84
13.70	0.30	2.00	4.53	4.93
14.00	0.30	2.00	4.44	5.53

In these tables,  $FS$  (P) indicates safety factor against pull out,  $FS$  (B) is safety factor against rupture of geotextile,  $L$  is length of the geotextile, vertical space is shown by  $S_v$  and  $Z$  represents the depth, which geotextile is placed.

### 3. Finite element modeling

According to present theories for the retaining walls sustainability issue, the vertical clay retaining walls are considered in a way that they could be stable with respect to their materials at static and non-reinforced states, with a safety factor a little greater than one. It is obvious that these retaining walls that suffer large deformation under seismic loads will be unstable (the numerical amount of these deformations were calculated by finite element method). On the other hand, reinforcing the retaining walls would increase their safety factor against static loads. Therefore, their behavior and relevant deformations under seismic loads were studied using the finite element method. Due to the role of reinforcing elements in controlling and restricting the deformations, the values of displacements, which were obtained in  $X$  and  $Y$  axes, completely guaranteed the retaining

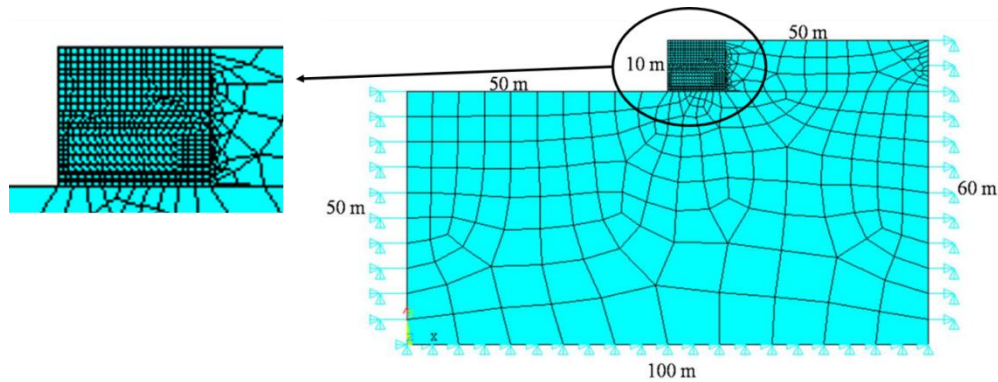


Fig. 3 The geometry of finite element model of 10-meter vertical wall

wall stability. A comparison was made between the two sets of deformations (horizontal and vertical displacements under seismic loading with and without reinforcing) at different heights of the walls, and the role of reinforcing elements in decreasing the displacement of the retaining wall was studied. Since the walls do not undergo any strain in longitude direction, two-dimensional finite element model was used to create plane strain condition. Fig. 3 shows the geometry of the finite element model for the 10-meter retaining wall as an example.

It is clear that specific points should be considered for defining  $\delta x$  and  $\delta y$ . Therefore, three points in the top, middle and bottom of the retaining wall were considered to evaluate the deformations.

### 3.1 Element type and boundary conditions

Fig. 4 shows the boundary conditions and the elements types which were used for modeling 10-meter reinforced retaining wall along with the optimized design of reinforced soil. As mentioned before, in this research, the horizontal and vertical displacements are evaluated, and due to the geometric damping, by taking distance from the wall, the movements gradually depreciate. The simplest solution to consider the effects of this damping is to use a large model in which the borders are so far from the wall that little vibration effects would reach to the borders (Jesmani *et al.* 2013, 2014). However, this method causes two problems: first, the enlargement of the model would lead to an increase in the amount of elements and nodes that were used in the computer model, and subsequently, freedom degrees of model, and practically, the number of calculations would increase, and as a result, the computer analysis would become too time consuming. On the other hand, considering that the lateral rigid borders will cause the problem of wave reflections from borders to the environment even if they were placed in far distance from the wall, and ultimately will create an unwanted condition of frequent back and forth of the wave in the system. To avoid these problems, the lateral borders were defined as spring-damper elements, and the entire system is formed by two sets of plane strain element and spring-damper elements along with the relevant contact elements (Barkan 1962).

To obtain more accurate results, elements were kept very small near the retaining wall, and by moving away from the wall they increased gradually in size. The geometry of FEM, meshing method and boundary conditions are shown in Fig. 3. As it can be seen, the mesh size in the model is very small close to the wall, and it increases by distancing from the reinforcements and the wall.

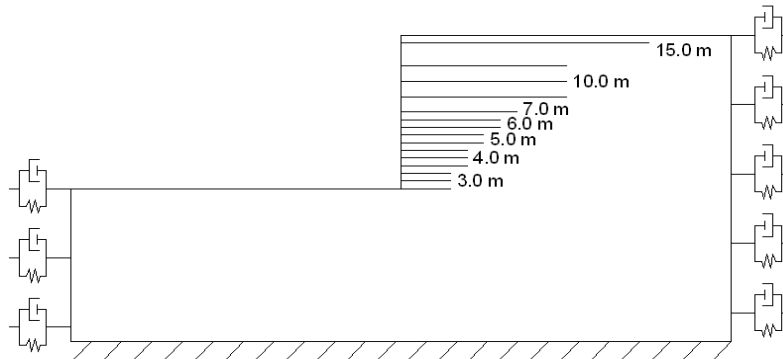


Fig. 4 Geometric scheme of the model and voundary condition of 10-meter reinforced clay vertical wall

The fine mesh sizing is extended in a way to completely cover the geotextile reinforcements' length in model. Considering the large size of the model and in order to have a more precise result, the model was meshed directly by the commands of the authors and created in the vicinity of the retaining wall (Jesmani *et al.* 2015). However, at the farther locations, automatic meshing system was used to mesh the model. This allowed calculating and obtaining the precise stress-strain behavior of the wall system at any desirable height.

3.1.1 Plane strain (PLANE82-2D 8) and spring-damper (COMBIN14) elements

Element Plane82 is a quadrille two-dimension element and could be easily used in square models with various sizes. This eight-noded element models the displacements fairly well, and in borders, it shows good behavior. This element is introduced by 8 nodes and each node has freedom degrees in both X and Y directions. This element is also able to model plastic behavior (Fig. 5(a)).

Fig. 5(b) shows the spring-damper element (SPD), which is a two dimensional, two-noded element. This element has the ability to model the linear and torsional springs. The SPD element has no mass, and by defining a mass element, its mass could be simulated. This element (SPD) is defined by the elastic coefficient of spring (K), linear and nonlinear damping coefficient (CV1 and CV2 respectively). In this research, to determine the elastic coefficient of spring, the elastic coefficient of soil was used, along with some experimental table and diagrams (Barkan 1962). The damping coefficient that has no effect on static loading was specified and defined for the dynamic loading as presented in different tables (Das 1993). In this element, the damping absolute values are somehow that the effects of wave reflection could be neglected.

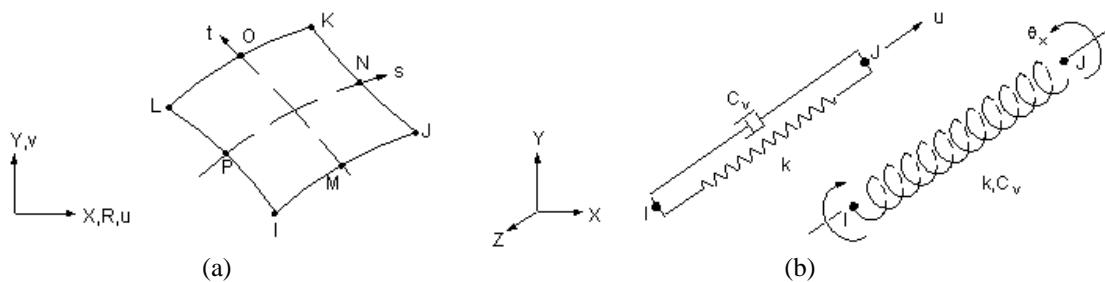


Fig. 5 Elements of the model: (a) Plane strain element; (b) Spring-damper element

### 3.2 Damping

The damping matrix  $[\mathbf{C}]$  used in harmonic, damped modal and transient analyses as well as substructure generation is defined as

$$[\mathbf{C}] = \alpha_r [\mathbf{M}] + (\beta_r + \beta_c) [\mathbf{K}] + \sum_{j=1}^{N_{mat}} \beta_j [\mathbf{K}_j] + \sum_{k=1}^{N_{EI}} [\mathbf{C}_k] + [\mathbf{C}_s] \quad (2)$$

where:

- $c_u$  : Cohesion of soil
- $[\mathbf{C}]$  : structure damping matrix
- $[\mathbf{M}]$  : structure mass matrix
- $[\mathbf{K}]$  : structure stiffness matrix
- $\alpha_r$  and  $\beta_r$  : Rayleigh damping
- $\beta_c$  : material-independent damping multiplier
- $\beta_j$  : material-dependent damping multiplier
- $N_{mat}$  : number of materials with DAMP input
- $N_{EI}$  : number of elements with specified damping
- $[\mathbf{K}_j]$  : portion of structure stiffness matrix based on material  $j$
- $[\mathbf{C}_k]$  : element damping matrix
- $[\mathbf{C}_s]$  : frequency-dependent damping matrix

In addition, the simplified form of damping matrix  $[\mathbf{C}]$  is calculated by multiplying the following constants to the mass matrix  $[\mathbf{M}]$  and stiffness matrix  $[\mathbf{K}]$

$$[\mathbf{C}] = \alpha_r [\mathbf{M}] + (\beta_r) [\mathbf{K}] \quad (3)$$

The Rayleigh damping is material-dependent damping ( $\beta_s$ ) calculated by Eq. (4).

$$\beta_s = \frac{\alpha_r}{2\omega_i} + \frac{\beta_r \omega_i}{2} \quad (4)$$

in which  $\omega_i$  donates the natural circular frequency of mode  $i$ .

In many practical soil related problems, alpha damping is ignored,  $\alpha_r = 0$ , (Jesmani *et al.* 2011) since it can lead to undesirable results, if a large mass has been introduced into the FE model. Assuming  $\beta_s = 0.05$ ,  $\alpha_r$  and  $\beta_r$  could be measured as following

$$\beta_r = \frac{0.05}{\pi f} \approx 5 \times 10^{-5}, \quad \alpha_r = 0 \quad (5)$$

where  $\pi$  is equal to 3.14 and  $f$  represent frequency.

### 3.3 Applied loads

Non-linear dynamic full transient analyses were performed to obtain the response of the model to the applied load (the San Jose earthquake loading). It should be noted that the San Jose earthquake is one of the typical seismic loading, which has been extensively investigated in

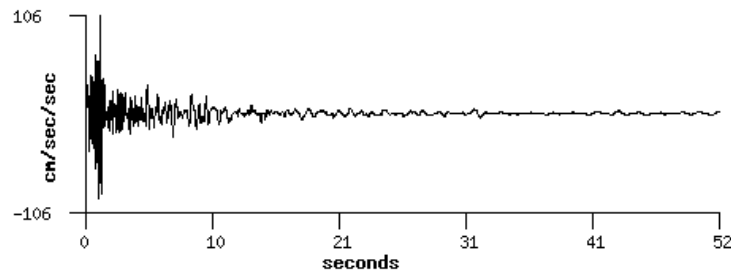


Fig. 6 Time-history loading of San Jose Earthquake

different researches and it has been the base of many previous studies (Cai and Bathurst 1995). The earthquake has occurred at San Jose, California, in 1955-09-05 at 02:01:18 UTC, and been recorded by different agencies such as “Consortium of Organizations for Strong-Motion Observation Systems”. The earthquake had a local magnitude (ML), commonly referred to as “Richter magnitude,” equal to 5.8, and happened at the depth of 0.0 km.

This load however, can be used in many studies with similar geological conditions to the San Jose area. These conditions could include the depth of bed rock, the thickness of alluvial layers, and type of fault. Therefore, in this research, this earthquake was selected as a time history for applying dynamic load on the model in which there were similar conditions to San Jose area (Fig. 6). The load of the earthquake has a specific time equal to 52 seconds and after that, with respect to the damping considered, the environment continues its vibration for a while. For assessing  $\delta x$  and  $\delta y$  in different time steps, the amount of these quantities were recorded during analysis, and their maximum values were chosen. In general, the results of analysis showed that  $\delta x_{max}$  and  $\delta y_{max}$  occurred when the seismic load (with respect to ground acceleration) has its maximum amount.

#### 4. Results and discussions

The horizontal and vertical displacements of several nodes at different locations on the wall were extracted from time history analyses for both reinforced and non-reinforced cases. By specifying the time variables (when maximum displacements occur) and the local variables (top, middle and bottom of the retaining wall), the values of  $\delta x$  and  $\delta y$  were evaluated for reinforced and non-reinforced walls with different heights. Fig. 7 shows the  $\delta x$  deformation counter in a specific time step for the 10-meter reinforced retaining wall as an example.

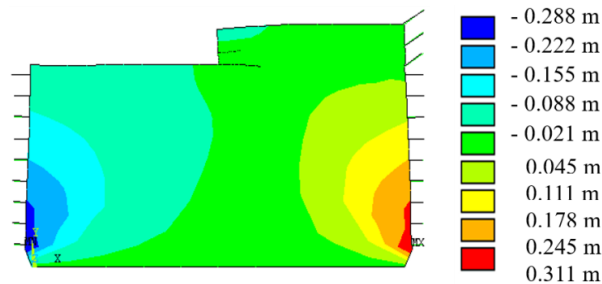


Fig. 7 Counter of strain of the 10-meter reinforced clay wall

The results of analysis indicate that the effects of the reinforcing system on the behavior of the retaining walls under dynamic load is very significant and it not only prevents stress concentration, but also it causes a suitable distribution of stress in soil mass and restricts the horizontal and vertical displacement in an acceptable range. However, no particular criterion exists to control deformations of reinforced walls, and controlling has been done merely by the relevant criteria of the gravity retaining walls; their behaviors are similar to the reinforced retaining walls. It should be mentioned that the gravity retaining walls displace rigidly while reinforced retaining walls relative deformation in height too. This should be considered and controlled in design procedure. It should also be mentioned that the Drucker-Prager yield criteria, which is one the most well-known and accepted criteria in geotechnical engineering, was considered for analyses in the finite element model.

#### 4.1 Effects of reinforcing on the displacement of retaining walls versus time

A comparison between the horizontal and vertical displacements of non-reinforced and reinforced retaining walls versus time was made and different deformations were calculated.

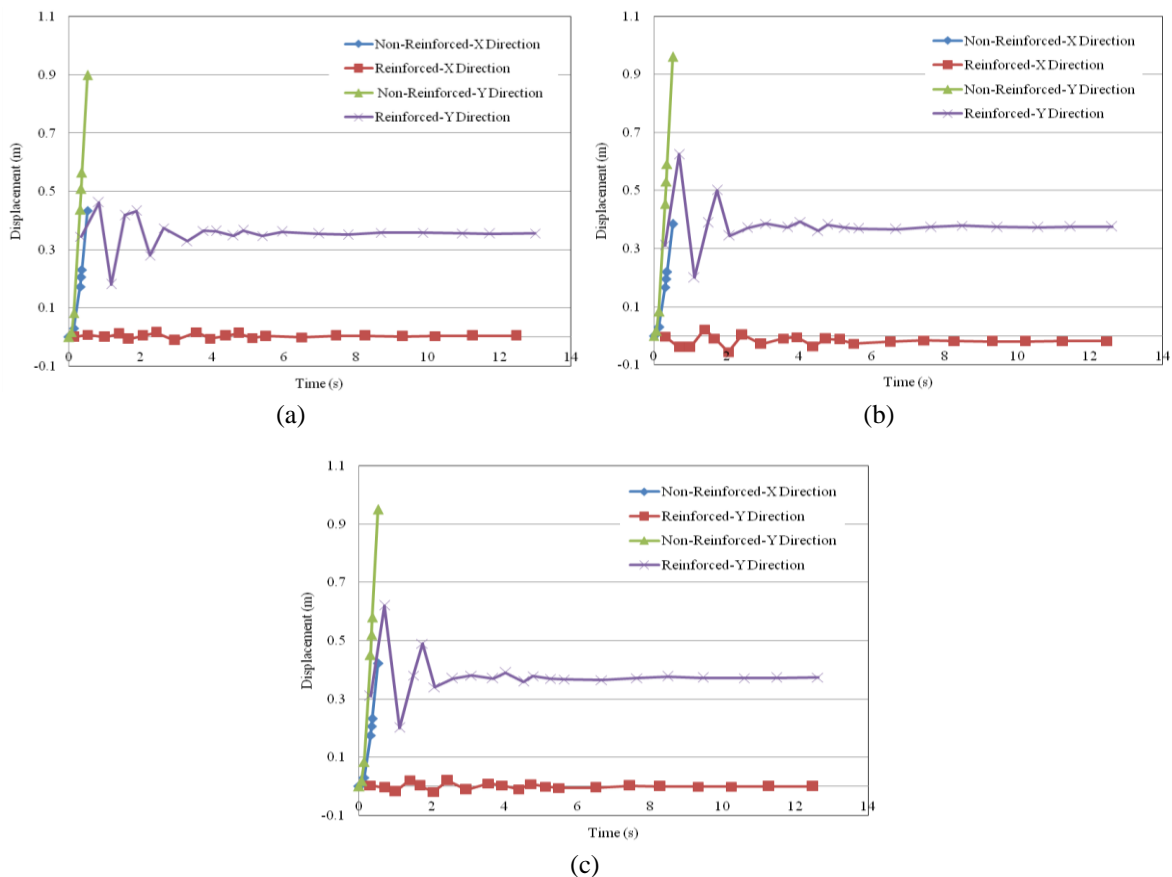


Fig. 8 Horizontal and vertical displacement of reinforced and non-reinforced 10 meter retaining wall versus time: (a) Top of the wall; (b) Middle of the wall; (c) Bottom of the wall

However, the displacements of 10-meter wall are presented as an example, in Fig. 8. It can be seen that the non-reinforced retaining wall will fail at about  $t = 1$  second. However, by reinforcing, it will sustain the earthquake load and will not fail during all dynamic load time.

In Fig. 8 outward horizontal displacement and downward vertical displacement of the wall are considered positive, and horizontal displacement toward the wall and upward vertical displacement are considered negative.

#### 4.2 Comparison between absolute displacements of reinforced and non-reinforced retaining walls

By considering the dynamic nature of seismic loads and changes that occur in quantity of load with time, it is obvious that  $\delta x$  and  $\delta y$  values (which indicate horizontal and vertical displacement respectively) show significant variation during the earthquake time. In addition, the amount of these displacements varied in different levels of wall. Therefore,  $\delta x$  and  $\delta y$  are practically studied as a two-variable function of time and location. Furthermore, due to considering two states of reinforced and non-reinforced retaining walls, it is practically noticed that there is a third parameter, reinforcing factor, (absence or existence) which is involved in the  $\delta x$  and  $\delta y$  quantity. Therefore, these quantities were considered as the most basic and important behavioral parameters of the walls.

To determine the amount of decrease in displacements of wall, which is the most significant index to describe the efficiency of reinforcement plan, the amounts of  $\delta x_{\max}$  and  $\delta y_{\max}$  (in most critical times that usually happens at the time of maximum acceleration) were extracted from the computer analysis at top, middle and bottom of the retaining walls. The results show that in non-reinforced conditions, value of displacements in general is too high and are in a range of 30cm to 57 cm for horizontal displacement and in a range of 82 cm to 90 cm for vertical displacement, showing large enough deformations to ruin the retaining walls. In reinforced retaining walls, the amount of  $\delta x$  is limited between 0.6 cm and 6.6 cm, and  $\delta y$  is limited between 27 cm and 38 cm. These numbers are in a low and acceptable range and guarantee the stability of the retaining wall during earthquake.

In order to study the variations of  $\delta x_{\max}$  and  $\delta y_{\max}$  in reinforced and non-reinforced retaining walls, different diagrams are presented. Fig. 9 shows the variations of maximum horizontal and vertical displacement in reinforced retaining walls compared to non-reinforced ones. It can be seen that by increasing the height of retaining wall from 6 m to 8 m, the value of  $\delta x_{R\max}$  increases. According to the Tables 3 and 4, it can be observed that the safety factor of the reinforcement design for both retaining walls is almost the same. Therefore, the main factor in appearance of horizontal deformation will be the height of the retaining wall; due to the higher height of 8 m retaining wall, the cantilever conditions of this wall and its freedom of movement has improved and caused greater displacement in x direction. At the same time, Tables 5, 6 and 7 show that by increasing the height of retaining wall from 8 m to 14 m, the relevant safety factors increase. Therefore, it has led to a decrease in the amount of  $\delta x_{R\max}$  along with increase in height of retaining wall, as is shown in Fig. 9. In fact, due to the relatively higher safety factor of reinforcement plan (in static loads conditions) for retaining walls higher than 10 m (Tables 5, 6 and 7) in comparison with lower retaining walls, 6 m to 8 m (Tables 3 and 4) the return of diagrams and reduction in horizontal displacement in taller retaining walls is predictable.

Fig. 9 clearly shows these results and is a confirmation of the effects of geotextiles in controlling and reducing horizontal deformation during earthquake, even in tall walls. Therefore, the significant and undeniable role of the safety factor of reinforcement plans in controlling

horizontal displacement is very clear. In addition, according to the existing procedures in reinforcing plan of retaining walls, usually the upper points of a retaining wall deform in a greater scale, and to prevent this problem, the length of geotextile must become longer in the upper points of a retaining wall (Fig. 4). Therefore, increasing the length of geotextiles in upper points of walls automatically causes better control on horizontal and vertical deformations in upper levels of the retaining wall. This could also be clearly seen in Fig. 9; however due to shorter lengths of geotextiles, values of  $\delta x_{Rmax}$  and  $\delta y_{Rmax}$  at lower parts of the retaining wall (its bottom) show higher values for horizontal and vertical displacement than the upper parts of the retaining wall. In other words, analyses reveal that in the reinforced retaining walls under seismic loading, the bottom of the wall experiences larger deformations than the middle and top of the wall due to smaller lengths of geotextiles. However, despite being stable, it seems that the length of geotextiles should be larger than the amount necessary for wall stability, and the suggestion of BS8006 (1995) about minimum reinforcement length at base of wall could be considered as a reliable amount.

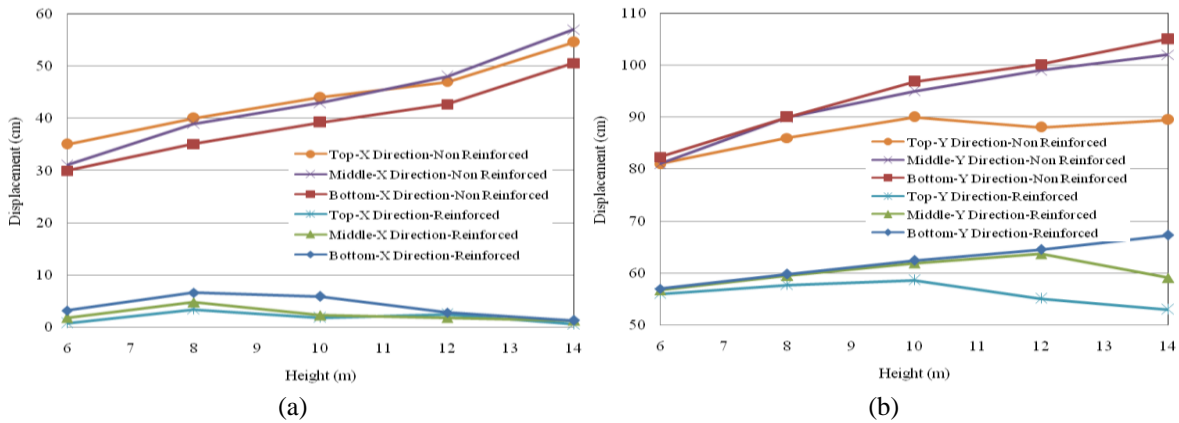


Fig. 9 Comparison of maximum displacement in reinforced and non-reinforced retaining wall: (a) Horizontal displacement; (b) Vertical displacement

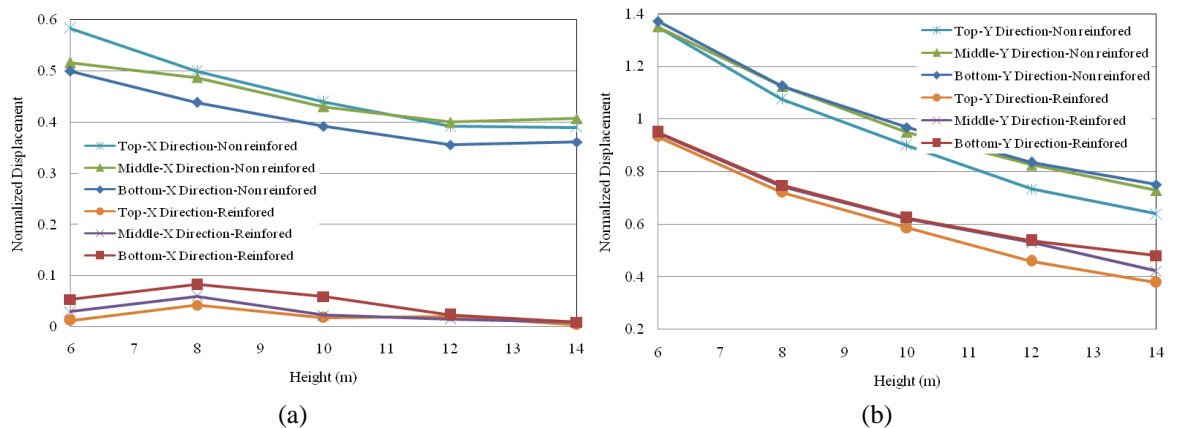


Fig. 10 Comparison of normalized maximum displacement in reinforced and non-reinforced retaining wall: (a) Horizontal displacement; (b) Vertical displacement

Table 8 Standard deviation of X and Y component of displacements

Height (m)	Standard deviation of X component of displacement			Standard deviation of Y component of displacement		
	Non-reinforced	Reinforced	NR / R	Non-reinforced	Reinforced	NR / R
6	2.67	0.99	2.70	0.31	0.18	1.72
8	4.73	1.72	2.75	2.48	0.86	2.88
10	5.15	3.34	1.54	7.23	2.84	2.55
12	4.56	0.18	25.33	33.55	18.11	1.85
14	6.02	0.11	54.72	48.69	34.33	1.42

\* NR/R represents the ratio of standard deviation of non-reinforced wall to reinforced wall

The general procedure of Fig. 9 shows that reinforcing the retaining wall controlled and limited the amount of displacement in the bottom, middle and top of the wall, and as the height of the retaining wall increases, it prevents deformations and keeps  $\delta x_{max}$  and  $\delta y_{max}$  relatively equable. However, due to generalization, horizontal and vertical displacement was normalized by height of the wall and are presented in Fig. 10. It can be seen that even though the higher retaining walls have larger displacements, the increment of the normalized displacements is less, and it can be concluded that higher retaining walls have lower normalized displacements.

In order to have a better concept of the effect of reinforcement on controlling the displacements, the dispersion of the amount of displacement at different levels in a wall with a specific height was calculated and the standard deviation of these data in reinforced and non-reinforced condition are presented in Table 8.

As can be seen, reinforcing the walls not only decreases the horizontal and vertical displacements, but also decreases the dispersion in the amount of deformation to a reasonable amount, and fewer scattering in data can be observed. However, the diagrams of the ratio of standard deviation of non-reinforced wall to reinforced wall are shown in Fig. 11.

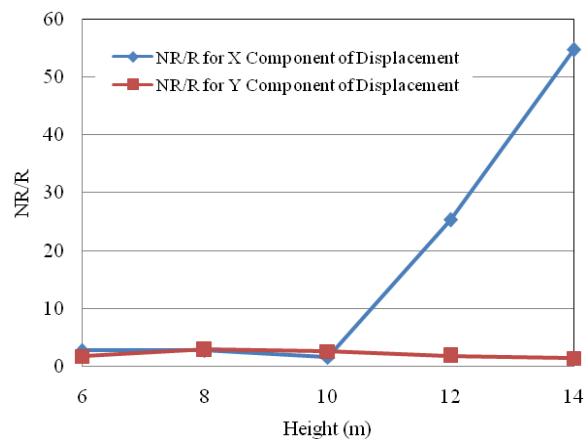


Fig. 11 Ratio of standard deviation of non-reinforced wall to reinforced wall for X and Y component of displacement

#### 4.3 Index of reduction for horizontal and vertical displacement ( $\Delta(\delta x_{max})\%$ and $\Delta(\delta y_{max})\%$ )

To evaluate the reinforcing effects on the most important behavioral parameter of retaining walls during earthquake (displacements), two dimensionless parameters are introduced to evaluate the amount of reduction in deformation. These parameters are defined in a way that could evaluate the effects of the reinforcing system at any specific time and points. Percent of displacement decrease in horizontal direction is defined by Eq. (6)

$$\Delta(\delta x_{max})\% = \frac{|\delta_{X NRmax}| - |\delta_{X Rmax}|}{|\delta_{X NRmax}|} \times 100 \quad (6)$$

in which

$\Delta(\delta x_{max})\%$  is decrease in horizontal displacement of reinforced status to non-reinforced status (Index of Reduction).

$\delta_{X NRmax}$  and  $\delta_{X Rmax}$  are maximum horizontal displacement in a specific height for non-reinforced and reinforced status respectively.

The same parameter could be introduced for vertical displacement ( $\Delta(\delta y_{max})\%$ ). To determine the quantity of index of reduction in horizontal and vertical displacement, the amounts of  $\Delta(\delta x_{max})\%$  and  $\Delta(\delta y_{max})\%$  (at the most critical time) are presented in Fig. 12. It can be seen that due to using geotextiles in optimized condition, the value of  $\Delta(\delta x_{max})\%$  decreased between 81% and 99% and the value of  $\Delta(\delta y_{max})\%$  decreased between 33% and 42% showing highly acceptable results in controlling the deformations.

As mentioned previously, in optimized conditions, the reinforcement plan shows a better effect in higher heights and taller retaining walls. At the same time, for a retaining wall with specific height, the highest and the lowest reduction are seen on the top and the bottom of wall respectively. These values could be reached to 99% and 42% for  $\Delta(\delta x_{max})\%$  and  $\Delta(\delta y_{max})\%$  in a 14 m retaining wall.

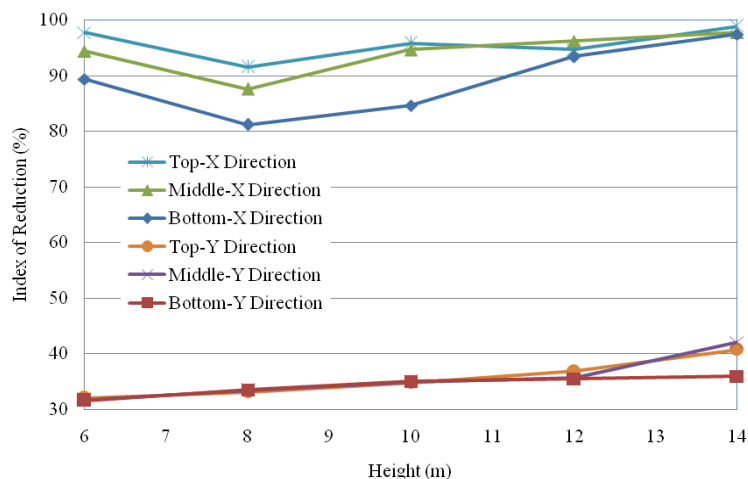


Fig. 12 Variation of the index of reduction of horizontal and vertical displacement versus the height of the retaining wall

Table 9 Normalized displacements formulas for non-reinforced retaining wall

Height	Normalized $X$ displacement formula	Normalized $Y$ displacement formula
Top	$X = 0.026H^2 - 0.761H + 9.335$	$Y = 0.149H^2 - 3.088H + 27.34$
Middle	$X = 0.025H^2 - 0.677H + 8.534$	$Y = 0.070H^2 - 2.206H + 24.45$
Bottom	$X = 0.029H^2 - 0.772H + 8.594$	$Y = 0.071H^2 - 2.210H + 24.51$

Table 10 Normalized displacements formulas for reinforced retaining wall

Height	Normalized $X$ displacement formula	Normalized $Y$ displacement formula
Top	$X = 0.137H^3 - 2.07H^2 + 13.44x - 31.45$	$Y = -0.003H^3 + 0.144H^2 - 2.567H + 20.22$
Middle	$X = 0.135H^3 - 2.08H^2 + 13.82x - 32.62$	$Y = -0.010H^3 + 0.342H^2 - 4.315H + 25.18$
Bottom	$X = 0.014H^3 - 0.35H^2 + 3.137x - 8.569$	$Y = -0.005H^3 + 0.212H^2 - 3.217H + 22.25$

Table 11 Index of reduction formulas

Height	$\Delta(\delta_{x_{\max}})\%$ formula	$\Delta(\delta_{y_{\max}})\%$ formula
Top	$\Delta(\delta_{x_{\max}})\%_{\text{Top}} = 1.10H^2 - 6.07H + 101.84$	$\Delta(\delta_{y_{\max}})\%_{\text{Top}} = 0.013H^3 - 0.30H^2 + 2.83H + 22.92$
Middle	$\Delta(\delta_{x_{\max}})\%_{\text{Mid}} = 0.79H^2 - 3.23H + 95.06$	$\Delta(\delta_{y_{\max}})\%_{\text{Mid}} = 0.061H^3 - 1.69H^2 + 15.67H - 14.85$
Bottom	$\Delta(\delta_{x_{\max}})\%_{\text{Bot}} = 2.13H^2 - 9.90H + 95.52$	$\Delta(\delta_{y_{\max}})\%_{\text{Bot}} = 0.003H^3 - 0.17H^2 + 2.853H + 19.72$

## 5. Mathematical formulation

According to the studies performed for the three different levels (bottom, middle and top) of the retaining walls, the mathematical formulas for the normalized displacement and index of reduction in horizontal and vertical displacement are introduced as a function of height of retaining wall ( $H$ ) in Table 9, 10 and 11. In these tables,  $X$  and  $Y$  represent the normalized horizontal and vertical displacement respectively.

Since the used parameters in the model, such as type of materials, geometry, geotextiles etc., are conventional in practical projects, the introduced formulas can be considered reliable for designing retaining walls. Design engineers could use these equations in design projects with similar reinforcement setting. The equations are of course mostly valid for the areas with similar geological conditions such as Northern California, Iran, Turkey, majority of Middle East, etc., but similar approach could be used to provide equations for other areas.

## 6. Conclusions

This paper has summarized the results of an investigation on the behavior of reinforced retaining walls with conventional heights, in which soil parameters are in the range of moderate and prevalent values of natural unsaturated clay that contains an amount of granular particles. The following specific conclusions can be drawn from the study:

- (1) Maximum displacements of vertical retaining walls under seismic loads usually occur in maximum accelerations of the load.
- (2) Common reinforcement plans in optimized conditions could decrease horizontal and

vertical displacements of retaining walls during earthquake up to 80% and 40% respectively.

- (3) Non-reinforced retaining walls during seismic loading usually experience the maximum horizontal displacement at crown, but the maximum vertical displacement would happen at the bottom and middle of the wall.
- (4) In the reinforced retaining walls under seismic loading, usually the maximum horizontal and vertical displacements occur at the bottom of the wall, and the minimum horizontal and vertical displacements, occur at top and middle levels of the wall.
- (5) Reinforcing the retaining walls can control and limit the difference of displacements at different points along the height of the wall. However, this controlling and limiting is more significant for displacement in  $X$  direction rather than  $Y$  direction. These values could be reached to 99% and 42% for  $\Delta(\delta x_{\max})$  % and  $\Delta(\delta y_{\max})$  % in a 14 m retaining wall.
- (6) Even though the higher retaining walls have larger displacements, the increment of their normalized displacements are smaller; therefore, the higher retaining walls have lower normalized displacements.
- (7) As the retaining wall height increases, the index of reduction increases and the soil reinforcement system shows more relative reduction in horizontal and vertical displacement; in other words, as the height of retaining wall increases, the efficiency of the reinforcement system become more significant.
- (8) In a retaining wall with a specific height, by increasing the level from bottom to top, the amount of index of reduction increases and it reveals that at higher levels of a retaining wall, the reinforcing system has more significant effects.
- (9) Despite being completely stable, it seems that the length of geotextiles at the base of reinforced retaining walls should be larger than the amount necessary for wall stability; the suggestion of BS8006 (1995) about minimum reinforcement length at base of wall can be considered a reliable amount.

## References

- AASHTO (1998), Interims: Standard specifications for highway bridges, *American Assoc. State Highway Trans. Officials*, Washington, D.C., USA.
- Barkan, D.D. (1962), *Dynamics of Bases and Foundations*, McGraw-Hill, New York, NY, USA.
- Bathurst, R.J., Allen, T.M. and Walters, D.L. (2005), "Reinforcement loads in geosynthetic walls and the case for a new working stress design method", *Geotext. Geomembr.*, **23**(4), 287-322.
- Bell, J.R., Stille, A.N. and Vandre, B. (1975), "Fabric retaining Earth walls", *Proceedings of the 13th Engineering Geology Soils Engineering Symposium*, Moscow, ID, USA.
- BS 8006 (1995), Code of practice for strengthened/reinforced soils and other fills; The British Standards Institution.
- Cai, Z. and Bathurst, R.J. (1995), "Seismic response analysis of geosynthetic reinforced soil segmental retaining walls by finite element method", *Compos. Geotech.*, **17**(4), 523-546.
- Das, B.M. (1993), *Fundamentals of Soil Dynamics*, PSW-Kent.
- Day, R.D. (2002), *Geotechnical Earthquake Engineering Handbook*, McGraw-Hill.
- Earthquake of San Jose 1955-09-05 02:01:18 UTC (1955), Consortium of Organizations for Strong-Motion Observation Systems (COSMOS), The Regents of the University of California.
- El-Emam, M.M. and Bathurst, R.J. (2007), "Influence of reinforcement parameters on the seismic response of reduced-scale reinforced soil retaining walls", *Geotext. Geomembr.*, **25**(1), 33-49.
- Elias, V., Christophere, B.R. and Berg, R.R. (2001), "Mechanically stabilized Earth walls and reinforced soil

- slopes design & construction guidelines”, FHWA-NHI-00-043; U.S. Department of Transportation Federal Highway Administration.
- FHWA (1996), “Mechanically stabilized earth walls and reinforced soil slopes design and construction guidelines”, (V. Elias and B.R. Christopher Eds.), *Federal Highway Admin. (FHWA) Demonstration Project 82*, Washington, D.C., USA.
- Gazetas, G., Psarropoulos, P.N., Anastasopoulos, I. and Gerolymos, N. (2004), “Seismic behavior of flexible retaining systems subjected to short-duration moderately strong excitation”, *Soil Dyn. Earthq. Eng.*, **24**(7), 537-550.
- GuhaRay, A. and Baidya, D.K. (2014), “Partial safety factors for retaining walls and slopes: A reliability based approach”, *Geomech. Eng., Int. J.*, **6**(2), 99-115.
- Holtz, R.D. and Lee, W.F. (2002), “Internal stability analyses of geosynthetic reinforced retaining walls”, Washington State Department of Transportation, WA-RD 532.1.
- Ismeik, M. and Shaqour, F. (2015), “Seismic lateral earth pressure analysis of retaining walls”, *Geomech. Eng., Int. J.*, **8**(4), 523-540.
- Jesmani, M., Kashani, H.F. and Kamalzare, M. (2010), “Effect of plasticity and normal stress on undrained shear modulus of clayey soils”, *Acta Geotech. Slovenica*, **1**, 47-59.
- Jesmani, M., Hamissi, A., Kamalzare, M. and Vileh, R.S. (2011), “Optimum geometrical properties of active isolation”, *Proceedings of ICE – Geotech. Eng.*, **164**(6), 385-400.
- Jesmani, M., Kamalzare, M. and Nazari, M. (2013), “Numerical study of behavior of anchor plates in clayey soils”, *Inter. J. Geomech., ASCE*, **13**(5), 502-513.
- Jesmani, M., Nabavi, S.H. and Kamalzare, M. (2014), “Numerical analysis of buckling behavior of concrete piles under axial load embedded in sand”, *Arab. J. Sci. Eng.*, **39**(4), 2683-2693.
- Jesmani, M., Kasrانيا, A., Kamalzare, M. and Mehdipour, I. (2015), “Undrained vertical bearing capacity of pile located near soft clay slope”, *J. Eng. Res.*, **3**(3), 21-38.
- Ji, J. and Liao, H. (2014), “Sensitivity-based reliability analysis of earth slopes using finite element method”, *Geomech. Eng., Int. J.*, **6**(6), 545-560.
- Koerner, R.B. (1986), *Design with Geosynthetics*, Prentice-Hall, Englewood Cliffs, N.J. Nation. Conc. Mason. Assoc. (NCMA), 1998, Segmental Retaining Walls - Seismic Design manual (Supplement to Design Manual for Segmental Retaining Walls authored by RJ Bathurst), Herdon, VA, USA, pp. 118-125.
- Lee, K.L., Adams, B.D. and Vagneron, J.J. (1973), “Reinforced Earth retaining walls”, *J. Soil Mech. Found., ASCE*, **99**(10), 745-763.
- Nian, T.K., Liu, B., Han, J. and Huang, R.Q. (2014), “Effect of seismic acceleration directions on dynamic earth pressures in retaining structures”, *Geomech. Eng., Int. J.*, **7**(3), 263-277.
- Okabe, S. (1924), “General theory on Earth pressure and seismic stability of retaining wall and dam”, *Doboku Gakkaishi – J. Japan Soc. Civil Eng.*, **10**(6), 1277-1323.
- Sabermahani, M., Ghalandarzadeh, A. and Fakher, A. (2009), “Experimental study on seismic deformation modes of reinforced-soil walls”, *Geotext. Geomembr.*, **27**(2), 121-136.
- Vidal, H. (1966), “La Terre Armee”, *Anales de l’Institut Technique du Batiment et des Travaux Publiques*, France, pp. 888-938.
- Yoo, C. and Kim, S.B. (2008), “Performance of a two-tier geosynthetic reinforced segmental retaining wall under a surcharge load: Full-scale load test and 3D finite element analysis”, *Geotext. Geomembr.*, **26**(6), 460-472.
- Zheng, D.F., Nian, T.K., Liu, B., Yin, P. and Song, L. (2015), “Coefficient charts for active earth pressures under combined loadings”, *Geomech. Eng., Int. J.*, **8**(3), 461-473.